Original Article

DOI: 10.7860/JCDR/2015/15035.6786

Pathology Section

Giant Cell Lesions of Lungs: A Histopathological and Morphometric Study of Seven Autopsy Cases

B.N KUMARGURU[1], M. NATARAJAN[2], DAYANANDA S BILIGI[3], A.R RAGHUPATHI[4]

ABSTRACT

Introduction: Macrophages undergo fusion to form multinucleated giant cells (MGC) in several pathologic conditions. The exact mechanism of their generation is still unclear. MGC are a common feature of granulomas that develop during various inflammatory reactions.

Aim: To study the histopathological features of giant cell lesions in lungs and correlate the characteristics of giant cells with other histopathological findings. Also, to determine the utility of morphometry to differentiate foreign body and Langhans MGC.

Materials and Methods: Seven cases were analysed. Specimen of lungs was grossed, sectioned and processed. Routinely, tissue sections were stained by Haematoxylin and Eosin (H&E) stain. Polarizing microscopy and special stains were employed in selected cases. Granulomas and MGC were counted and measured. Several other parameters like location, distribution, type and number of MGC, associated predominant inflammatory component and nature of granulomas were analysed.

Results: Five patterns of lesions were observed in seven cases. Aspiration pneumonia was seen in three cases (42.85%) and constituted the most common pattern. However, aspiration pneumonia as the only cause of MGC was seen in only one case (14.28%). Pulmonary tuberculosis and asteroid bodies constituted two cases (28.57%) each. Cryptococcal pneumonia and cholesterol clefts constituted one case (14.28%) each. Crypococci were demonstrated to be positively birefringent by polarized microscopy on Ziehl-Neelsen stained sections. Based on statistical analysis of morphometric data, a new index (NP index) was proposed to statistically categorize MGC into foreign body type and Langhans type. NP index value of ≤0.016 was found to be statistically significant ($p<0.005$) in foreign body MGC. It had high sensitivity and efficacy.

Conclusion: MGC may not be always associated with granulomas. The mechanisms that lead to the occurrence of MGC, independent of granuloma needs to be elucidated. Morphometry may serve as a useful aid. But a pathologist has to rely on the morphological details to categorize MGC.

Keywords: Multinucleated giant cells, Granulomas, Cryptococci, Birefringent

INTRODUCTION

Multinucleated giant cells (MGC) are considered to originate from the fusion of monocyte-macrophage lineage cells [1]. Formation of these giant cells is believed to enhance the defensive capacities of macrophages [2]. Morphologically, MGC are generally classified into Langhans giant cells or foreign body giant cells (FBGC). Langhans MGC are commonly seen in immune granulomas with epithelioid macrophages [1]. FBGC formation from the fusion of macrophages is observed as a result of response induced by biomaterials and other foreign bodies [2]. MGC phenotypes vary, depending on the local environment and the chemical and physical (size) nature of the agent to which the MGC and their monocyte/macrophage precursors are responding [3].

MGC are a common feature of granulomas that develop during various inflammatory reactions [4] stimulated by both immunological and non-immunological stimuli [5]. Granulomas in pulmonary pathology often pose a diagnostic challenge [6]. MGC are prominent feature of some chronic inflammatory states in the lungs. Alveolar macrophage proliferation appears to be prerequisite for cell fusion and MGC formation as a feature of granulomatous disease [7].

AIM

The current study was undertaken to evaluate the histological features of giant cell lesions of lungs, correlate the characteristics of giant cells with other histopathological finding and to determine the utility of morphometry to differentiate the foreign body and Langhans giant cells.

MATERIALS AND METHODS

The study was done from November 2009 to March 2011. In the present study, seven cases were analysed. During the study period, from a total of 231 cases, lung specimens were received in 136 cases among the other organs sent for histopathological examination. Only those cases which showed giant cells in histopathological sections of lungs were included in the study. Rest of the cases in which MGC were not appreciated were excluded from the study and constituted 129 cases. Specimen of lungs was grossed, sectioned and processed as per standard operating procedure. Routinely tissue sections were stained by Haematoxylin and Eosin (H&E) stain. However special stains like Periodic acid Schiff (PAS), toludine blue (TB), Reticulin silver, Ziehl-Neelsen (ZN) and Phosphotungstic acid haematoxylin (PTAH) were employed in selected cases. Sections were examined in polarizing microscope in selected cases. Granulomas were counted under scanner and measured. MGC were counted under scanner, measured in high power and examined in each case. Several other parameters like location, distribution, associated predominant inflammatory component, type and number of MGC and the nature of granuloma were analysed.

Measurement of granuloma, MGC, special structures such as fungi or asteroid bodies was done by software “Prog Res® capture Pro 2.6”. Short axis and long axis of each structure was measured and expressed in micrometer. All giant cell lesions of lungs were correlated with available history, autopsy findings and histopathological findings of lungs and other organs received. All statistical calculations were

done using Microsoft office excel 2007 and R 3.2.1 software. Fisher-exact test was used to find out the significance of morphometric data of MGC and statistically categorize MGC into foreign body type and Langhans type.

RESULTS

In the present study, seven cases (5.1%) of giant cell lesions of lungs were analysed [out of 136 cases in which the lung specimens were received]. Their ages ranged from 20 to 60 years with a mean of 39.42 years. From a total of seven cases, specimens of lungs were sent in 2 pieces in 6 cases (85.71%) and whole of right lung was sent in one case (14.28%). Five patterns of lesions were observed in seven cases. Aspiration pneumonia was seen in three cases (42.85%) and constituted the most common pattern. However, aspiration pneumonia as the only cause of giant cells was seen in only one case (14.28%). Pulmonary tuberculosis and asteroid bodies were associated with MGC in two cases (28.57%) each. Cryptococcal pneumonia and cholesterol crystals constituted one case (14.28%) each. The distribution of giant cell lesions is shown in [Table/Fig-1] and the summary of histological characteristics of giant cells is depicted in [Table/Fig-2].

Case Number	Age (Y)	Sex	History	Primary Histological Feature	Secondary Histological Findings
1	60	Male	Road traffic accident	Cryptococcal pneumonia	Aspiration pneumonia
2	25	Male	Custodial death	Cholesterol clefts	Congestion and edema
3	28	Female	Hanging	Pulmonary tuberculosis	Aspiration pneumonia
4	50	Female	Snake bite	Asteroid body	Congestion
5	45	Male	Respiratory tract infection	Asteroid body	Congestion and edema
6	48	Male	Snake bite	Aspiration pneumonia	Congestion and edema
7	20	Female	Criminal negligence	Pulmonary tuberculosis	Patchy pneumonia

[Table/Fig-1]: Distribution of Giant cell lesions of lungs

Histological Feature in giant cell lesions	Number of cases	Predominant type of giant cell	Highest number of giant cells per scanner field	Highest number of nuclei in a giant cell	Long axis of largest giant cell in microns
Pulmonary tuberculosis	2 (28.57%)	Langhans type	5	22	103.2
Asteroid bodies	2 (28.57%)	Foreign body type	9	14	73.49
Aspiration pneumonia	1 (14.28%)	Foreign body type	1	17	72.16
Cryptococcal pneumonia	1 (14.28%)	Langhans type	1	16	52.36
Cholesterol clefts	1 (14.28%)	Foreign body type	6	29	90.09

[Table/Fig-2]: Histological characteristics of giant cells

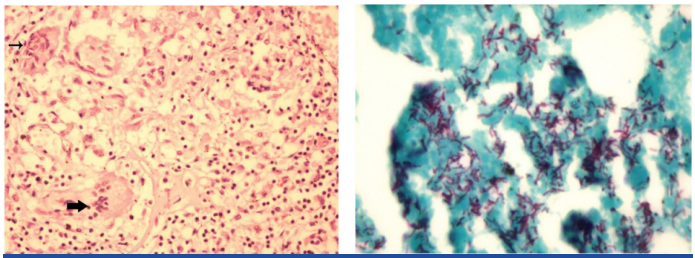

[Table/Fig-3]: Microphotograph of tissue section of lung displaying Langhans type (thick arrow) and foreign body type of giant cells (thin arrow) in a case of pulmonary tuberculosis (case 3). (H&E, X200) **[Table/Fig-4]:** Microphotograph of tissue section of lung displaying acid fast bacilli in a case of pulmonary tuberculosis (case 3). (ZN, X1000)

Pulmonary tuberculosis: MGC were appreciated in two cases (case 3 and case 7) of pulmonary tuberculosis. One case (case 3) was associated with aspiration pneumonia while the other case (case 7) was associated with patchy pneumonia. Case 3 was associated with history of hanging while case 7 was associated with criminal negligence. Both the cases showed granulomas distributed diffusely throughout the parenchyma. Case 3 showed four granulomas per scanner while case 7 showed nine granulomas per scanner and constituted highest number of granulomas seen per scanner in the present study. Largest granuloma in case 3 measured 531.9 µm in its long axis. Largest granuloma in case 7 measured 2114.21 µm in its long axis.

Case 3 showed MGC in 3 (75%) granulomas in scanner, one MGC in each granuloma. Two MGC were of Langhans type. One was of foreign body type [Table/Fig-3]. They were located peripherally within the granuloma. Largest MGC measured 103.20 µm in its long axis. Mean long axis measurement was 70.04 µm. Nuclei of some giant cells were translucent (66%) while others were hyperchromatic (33%). The number of nuclei varied from 9 to 22 with an average of 15 nuclei in each MGC. Granulomas were not associated with

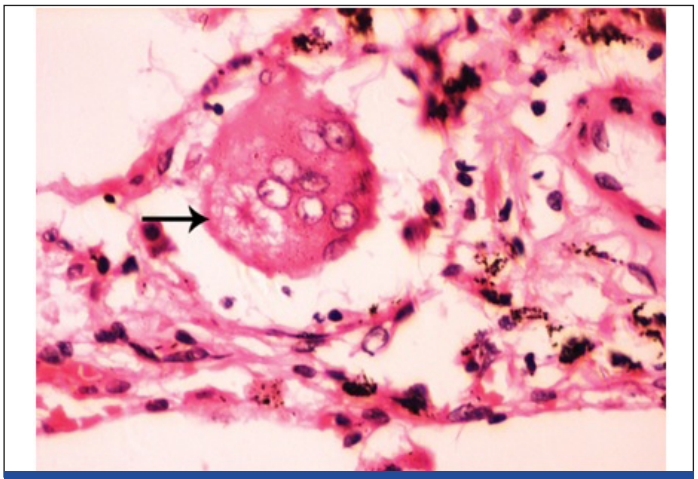

[Table/Fig-5]: Microphotograph of tissue section of lung displaying foreign body type of giant cells (arrow) with asteroid body (case 5). (H&E, X400)

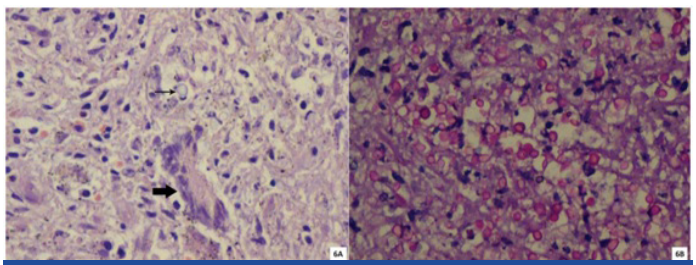

[Table/Fig-6a]: Microphotograph of tissue section of lung displaying Langhans type of giant cell (thick arrow) and Cryptococci (thin arrow) in a case of cryptococcal pneumonia (case 1). (H&E X200)
[Table/Fig-6b]: Microphotograph of tissue section of lung displaying capulated cryptococci in a case of cryptococcal pneumonia (case 1). (PAS, X200)

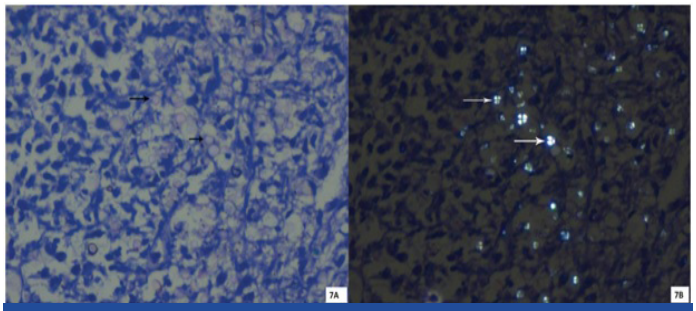

[Table/Fig-7a]: Microphotograph of tissue section of lung displaying cryptococci (arrows) in a case of cryptococcal pneumonia (case 1) before polarization. (ZN, X200)
[Table/Fig-7b]: Microphotograph of tissue section of lung displaying birefringent cryptococci (arrows) with maltese cross appearance in a case of cryptococcal pneumonia (case 1) after polarization. (ZN, X200)

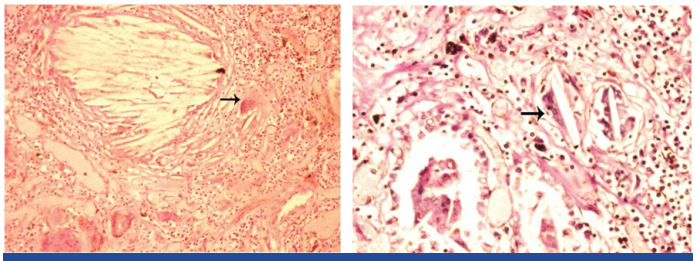

[Table/Fig-8]: Microphotograph of tissue section of lung displaying aggregates of cholesterol clefts with surrounding foreign body giant cells (arrow) in case 2. (H&E, X100)
[Table/Fig-9]: Microphotograph of tissue section of lung displaying foreign body giant cells with engulfed cholesterol cleft (arrow) in case 2. (H&E, X200)

caseation necrosis. However, acid fast bacilli were seen in ZN stained sections [Table/Fig-4]. Similar granulomas were appreciated in liver and mesenteric lymph node sections.

Case 7 showed MGC in 5 (55%) granulomas in scanner. MGC were located peripherally within the granuloma. 3 MGC were of foreign body type and 2 MGC were of Langhans type. Largest MGC measured 48.02 µm in its long axis. Mean long axis measurement was 36.41 µm. The number of nuclei varied from four to nine in each MGC. Nuclei were translucent. Granulomas were associated with caseation necrosis. Acid fast bacilli were seen in ZN stained sections. At places lungs showed foci of neutrophilic infiltration. Similar granulomas were appreciated in brain, liver, spleen and mesogastric lymph node sections.

Asteroid bodies: MGC were associated with asteroid bodies in two cases (case 4 and case 5). Case 4 did not have significant histopathological findings while case 5 was diagnosed to have multiple myeloma. Case 4 was seen in a female in sixth decade and presented with history of snake bite while the deceased was working in areca nut farm. Case 5 was seen in a male in fifth decade and presented with history of respiratory tract infection. The deceased was on ayurvedic treatment. In both the cases, MNG were not associated with granuloma.

In case 4, maximum of 8 MGC were appreciated in scanner. MGC were located in the lung parenchyma and hilar lymph nodes. All MGC were of foreign body type. Largest MGC measured 65.85 µm in its long axis. Mean long axis measurement was 46.04 µm. The number of nuclei varied from four to eleven with an average of six nuclei in each MGC. Nuclei were translucent in all the MGC.

Maximum of 5 (62.5%) MGC showed asteroid bodies in scanner. Largest asteroid body measured 22.81 µm. They were appreciated as small round bodies with tentacles emerging the body. All asteroid bodies were located within MGC pushing the nuclei to the periphery. Lymphocytes and eosinophils were seen around MGC. Asteroid bodies were appreciated in H&E, toludine blue, PAS and PTAH stained sections. Sections from heart showed evidence of fresh myocardial infarction and left coronary atherosclerosis.

In case 5, maximum of nine MGC were observed in scanner and constituted the highest number of MGC seen in scanner in the present study. All the MGC were of foreign body type [Table/Fig-5]. Nuclei were translucent. Largest MGC measured 73.43 µm in its long axis. Mean long axis measurement was 51.67 µm. The number of nuclei varied from four to fourteen with an average of eight nuclei in each MGC. Giant cell reaction was associated with lymphocytic infiltration. Maximum of 2 (22.19%) MGC showed asteroid bodies in scanner. The morphology and staining characteristics were similar to those of case 4. Skull vault and rib mass that were sent showed evidence of multiple myeloma. However, lungs were not involved by the neoplasm.

Aspiration pneumonia: Aspiration pneumonia was seen in three cases (case 1, case 3 and case 6). Case 1 was associated with history of road traffic accident. Case 3 was associated with history of hanging. Case 6 was associated with history of snake bite.

Aspiration pneumonia was an associated finding in case1 (cryptococcal pneumonia) and case 3 (pulmonary tuberculosis). In case 6, aspiration pneumonia was the only finding associated with giant cell lesion of lungs. Only one MGC was noted in scanner. It was of foreign body type and measured 72.16 µm in its long axis. MGC was not associated with any granulomas. The nuclei were 17 in number and were translucent in nature. Neutrophils constituted predominant inflammatory component associated with the lesion. Sections studied from skin showed foci of neutrophilic infiltration in stratum corneum.

Cryptococcal pneumonia: MGC was appreciated in a case of cryptococcal pneumonia. The deceased was a 60-year-old male with history of road traffic accident. The lesion was associated with evidence of aspiration pneumonia. Sections from lungs showed granulomatous reaction surrounded by fibrocollagenous tissue. Granuloma measured 2593 µm in its long axis and it constituted largest granuloma in the present study. Langhans type of MGC was seen in the periphery of the granuloma [Table/Fig-6a]. MGC measured 52.36 µm in its long axis. Nuclei were hyperchromatic and were 16 in number. The centre of granuloma showed abundant neutrophils and necrotic material. Inflammatory component constituted neutrophils predominantly followed by epithelioid cells, lymphocytes, plasma cells and fibroblasts. Amidst the necrotic area and neutrophils, numerous cryptococci (60-80/oil immersion field) were seen, varying in size from 2.75 µm to 6.53 µm with an average of 4.6 µm in long axis. The fungi showed budding yeast forms. Cryptococcal capsule was well appreciated in PAS [Table/Fig-6b] and reticulin stained sections. Furthermore, many cryptococci were positively birefringent under polarizing light. Positive birefringence was better appreciated in ZN stained sections than toludine blue stained sections. Cryptococci showed internal budding and maltese cross appearance [Table/Fig-7a,b]. However, not all forms were positively birefringent. Probably only the younger forms exhibited birefringence. The granuloma was an incidental finding. Sections from heart revealed evidence of old infarction and left coronary atherosclerosis.

Cholesterol clefts: MGC associated with cholesterol clefts was appreciated in a case of custodial death in a 25-year-old male. MGC was not associated with granulomas. Cholesterol clefts were seen in aggregates [Table/Fig-8] which measured 405.9 µm. Also, seen were scattered cholesterol clefts. On an average, individual cholesterol cleft measured 63.9 µm in its long axis. Maximum of six MGC were seen in scanner. MGC were located at the periphery of cholesterol clefts [Table/Fig-9]. Largest MGC measured 90.09 µm in its long axis. Mean long axis measurement was 61.75 µm. Out of six MGC, five (83.33%) were foreign body type and one (16.66%) was of Langhans type. The nuclei were translucent and varied in number from six to twenty nine with an average of 13 nuclei in each MGC. Twenty nine nuclei per MGC constituted the highest number of nuclei in a MGC in the present study. Inflammatory components constituted predominantly lymphocytes followed by macrophages, eosinophils and neutrophils. Special stains did not contribute to any additional information. Sections from rest of lungs showed only congestion and edema. Sections from heart showed atherosclerosis of left coronary artery. Sections from liver showed evidence of cirrhosis. Sections from kidney showed features of acute tubular necrosis.

Morphometric analysis: Morphometric analysis was performed on 33 MGC [which included 27 foreign body giant cells and 7 Langhans type] to differentiate between the two types of giant cells. The number of nuclei in the MGC varied from four to twenty-nine nuclei in foreign body type and ranged from nine to twenty-two nuclei in Langhans type. In foreign body giant cells, short axis measurement ranged from 16.79µm to 58.49µm and long axis measurement ranged from 23.79µm to 90.09µm. In Langhans giant cells, short axis measurement ranged from 15.7µm to 44.8µm and

long axis measurement ranged from 52.96µm to 103.2µm. Based on statistical analysis (Fisher exact test) of morphometric data, a new index (NP index) was proposed to statistically categorize MGC into foreign body type and Langhans type. NP index was defined as ratio of number of nuclei in MGC (N) to product of long axis and short axis (P). Last four digits after the decimal point was considered for expressing NP index. In foreign body MGC, product of long axis and short axis (P) varied from 399.4341 μm^2 to 5269.3641 μm^2 and NP index ranged from 0.0018 to 0.0158. In Langhans giant cell, Product of long axis and short axis (P) varied from 504.5144μm^2 to 4623.36μm^2 and NP index ranged from 0.0019 to 0.2515. For statistically identifying foreign body MGC, NP index had very high sensitivity (100%), low specificity (57.14%) and High efficacy (90.90%). NP index value of ≤ 0.016 was considered to categorize a MGC as foreign body giant cell. Similarly NP index value of > 0.016 was considered to categorize a MGC as Langhans type. NP index value of ≤ 0.016 was found to be statistically significant (p <0.005) in foreign body giant cells. Based on only number of nuclei in MGC (> 20 nuclei for foreign body giant cells), statistical identification of foreign body MGC was found to be insignificant (p = 0.384).

DISCUSSION

MGC originate from fusion of monocytes or macrophages, but little is known about the mechanisms of fusion. Furthermore, it is not clear how monocyte fusion is induced in vivo and whether different mechanisms are involved in different pathological states [1]. MGC are formed as a result of cell fusion rather than abnormal cell division [8]. Alveolar macrophage fusion occurs as a post-mitotic event. Invitro studies suggest inverse relationship between cell fusion and proliferation [7]. Human serum is known to induce maturation of human monocytes into macrophages in vitro. Monocytes' antimicrobial activity declines during maturation. Fusion with monocytes could be of benefit for macrophages that have taken up certain bacteria or parasites [4]. Epithelioid cells containing vesicles develop in damaged and necrotic areas and mainly this type of epithelioid cell fuses to form giant cells [9]. MGC are a common feature of granulomas that develop during certain infections, most prominent example being tuberculosis or as a consequence of foreign body reactions (FBR) [4]. Using various animal models, in vivo and invitro studies have suggested that initiation, maintenance, and resolution of granulomatous inflammations are dependent on soluble T-cell factors [8].

Pulmonary tuberculosis: In the present study, two cases of pulmonary tuberculosis were documented. Karimi S et al., documented granulomas in five lung specimen (21.7%) [10]. MGC were seen in five cases out of 23 cases. However, exact proportion of cases showing MGC in lung tissues and their details were not specified in their study.

The presence of MGC in the tuberculosis granuloma was first described by Langhans in 1868 [1]. Langhans MGC were the predominant type of giant cells in case 3 while FBGC was predominant in case 7. Interleukin (IL)-4 or IL-13 induction of monocyte-macrophage fusion provides a model for FBGC formation. Interferon-γ induction of monocyte-macrophage fusion provides a model for Langhans MGC formation. Although FBGC, Langhans MGC and osteoclasts are derived from monocytes or monocyte progenitor cells, the ways in which they are formed, whether induced by cytokines, receptors or biologic activity, are markedly different [1].

Asteroid bodies: In the present study, two cases showed presence of asteroid bodies within MGC in the lungs. Asteroid body was seen in a case of multiple myeloma (Case 5). However, lungs did not show any evidence of tumour involvement. Exact aetiology of the other case (case 4) remained obscure. Asteroid bodies are intracytoplasmic inclusions, thought to represent endogeneous products of macrophage metabolism [6]. These are commonly seen in sarcoidosis, sporotrochosis and FBGC reactions [11]. Winkelmann RK et al., observed asteroid body in skin biopsy specimens of 8 cases (33%) out of the 24 patients with Necrobiotic xanthogranuloma with paraproteinaemia [12]. Gadde PS et al., observed asteroid bodies in two lung specimens (22%) [11]. Both the cases were associated with sarcoidosis. They concluded that asteroid bodies constitute products of unusual centrosome-microtubule organizing center dynamics in MGC [11].

Cryptococcal pneumonia: In the present study, Langhans MGC with solitary caseating granuloma was seen in tissue section of lungs in a case of cryptococcal pneumonia. Gazzoni AF et al., reported four cases (30%) of cryptococcal infection in lung tissue [13]. MGC included both Langhans type and foreign body type in their study. Baker RD et al., described nine cases of cryptococcal infection predominantly involving lung tissue among 26 cases [14]. Various tissue reactions constituted polymorphonuclear leukocytic infiltration (11cases), lymphocytic response (22 cases), giant cells (23 cases), caseation necrosis (four cases) and fibrosis (15 cases). Similar tissue reactions were observed even in the present case.

Cholesterol clefts: In the present study, MGC associated with cholesterol cleft was seen in a case of custodial death. MNG included foreign type (predominantly) and Langhans type. The exact cause of death could not be determined in the present case. Sabastine MS et al., reported a case of pulmonary cholesterol crystal embolisation [15]. Giant cell reaction was not described in their case. Within 48 hours, a FBGC reaction may occur resulting in engulfment of cholesterol crystals. Possible causes of embolization are presence of arterio-venous shunt or pulmonary artery atheroma.

Aspiration pneumonia: In the present study, MGC associated with aspiration pneumonia as primary diagnostic finding constituted a single case. However, aspiration pneumonia was associated feature in pulmonary tuberculosis and cryptococcal granuloma. Horacek J et al., reported a case of granulomatous reaction with MGC formation in lungs secondary to aspiration of vegetable particles (maize starch) [16]. A variety of substances, including oropharyngeal bacteria, foreign bodies, milk, barium, exogenous lipids and gastric contents can be aspirated into the lungs, leading to a wide range of tissue reactions and clinical consequences. In the most classic cases, it is associated with acute inflammation and/ or foreign body granulomas or MGC containing aspirated foreign material. Presence of particulate foreign material is the key diagnostic finding [6]. The process centres around bronchioles, which may be destroyed and replaced by acute inflammation and necrosis [17].

IFN-γ is the essential factor promoting monocyte fusion [4]. Recent report implicates TNF-α involvement in multinucleation of macrophages [7]. Matrix metalloproteinase-9 (MMP-9) is the first secreted extracellular enzyme shown to participate in macrophage fusion. MMP-9 has potential to modulate FBGC formation. Interestingly, in an invitro model of granuloma-associated macrophage fusion, it was shown that the process requires a disintegrin and metalloprotease domain 9 (ADAM 9) [2]. IL-4 may induce formation of multinucleated cells by interfering with normal cell division. IL-4 acts directly on monocytes to promote fusion and does not secondarily induce production of other soluble fusion factors. IL-4 also causes aggregation of macrophages and diminishes their migration [8]. FBGC most commonly are observed at tissue/material interface of implanted medical devices, prostheses, and biomaterials. Adherent macrophages and FBGC constitute foreign body reaction. FBGC are also seen in tissues where the size of foreign particulate is too large to permit macrophage phagocytosis [3].

Langhans MGC are associated with indigestible particles of organisms surrounded by a collar of mononuclear leukocytes, principally lymphocytes. It was stated that the Langhans MGC are characterized by a relatively small number of nuclei, generally less than 20, arranged in a circular peripheral arrangement within MGC and FBGCs generally have more nuclei, greater than 20,

arranged in irregular fashion throughout MGC [1]. However, in the present study, there was no such correlation between the number of nuclei and the type of MGC. MGC with high numbers of nuclei per cell, produced by highly virulent mycobacteria are considered as the final stage of formation and/or differentiation of MGCs. These cells are incapable of phagocytosis but still retain a strong antigen presentation capability [9].

Based on only number of nuclei in MGC (> 20 nuclei for foreign body giant cells), statistical identification of foreign body MGC was found to be insignificant. On the contrary, NP index value of ≤ 0.016 was found to be statistically significant in foreign body giant cells. NP index had very high sensitivity, low specificity and high efficacy. Florez-Moreno GA et al., utilized cytomorphometry to differentiate central giant cell lesion and peripheral giant cell lesion of jaw based on the number and nuclear size in their study [18]. The nuclei in central giant cells lesions were more numerous, larger and more irregular than those in peripheral giant cells lesions. Anderson S et al measured the size of MGC and number of nuclei within the MGC in their study, but categorization was not mentioned [19]. Statistical values may vary among different studies. Morphometry may be a useful aid. But a pathologist has to rely on the morphological details to differentiate or categorize MGC. The characterization of a multinucleated giant cell needs not only the number of nuclei and measurement of the giant cell, but also the position of nuclei and presence or absence of engulfed particle.

CONCLUSION

Giant cell lesions in lungs may have diverse aetiopathogenesis. MGC may not be always associated with granulomas. The molecular mechanism involved in lesions with MGC in association with granuloma may be different from lesions with only giant cells without granuloma. The mechanisms that lead to occurrence of MGC independent of granulomas needs to be elucidated by molecular studies. The statistical significance of morphometric data may vary among different studies. Morphometry may serve as a useful aid. But a pathologist has to rely on the morphological details to categorize MGC.

ACKNOWLEDGMENT

We sincerely thank Department of Forensic Medicine, BMCRI, Bangalore, Karnataka for the kind cooperation extended to us in the work up of cases. We also thank the statistician, Department of Community Medicine, PESIMSR, Kuppam, Andhra Pradesh for the kind help extended to us for statistical analysis.

REFERENCES

[1] Anderson JM. Multinucleated giant cells. *Curr Opin Haematol*. 2000;7:40-47.
[2] MacLauchlan S, Skokos EA, Meznarich N, Zhu DH, Raoof S, Shipley JM, et al. Macrophage fusion, giant cell formation, and the foreign body response require matrix metalloproteinase 9. *J Leukoc Biol*. 2009;85:617–26.
[3] Brodbeck WG, Anderson JM. Giant cell formation and function. *Curr Opin Haematol.* 2009;16:53–57.
[4] Most J, Spotl L, Mayr G, Gasser A, Sarti A, Dierich MP. Formation of Multinucleated Giant Cells Invitro Is Dependent on the Stage of Monocyte to Macrophage Maturation. *Blood*. 1997;89:662-71.
[5] Postlethwaite AE, Jackson BK, Beachley EH, Kang AH. Formation of multinucleated giant cells from human monocyte precursors. Mediation by a soluble protein from antigen- and mitogen-stimulated lymphocytes. *J Exp Med*. 1982;155:168-78.
[6] Mukhopadhyay S, Gal AA: Granulomatous lung disease, an approach to differental diagnosis. *Arch Pathol Lab Med*. 2010;134:667-90.
[7] Prieditis H, Adamson IY. Alveolar macrophage kinetics and multinucleated giant cell formation after lung injury. *J Leukoc Biol*. 1996;59:534-38.
[8] McInnes A, Donna M. Rennick DM. Interleukin 4 induces cultured monocytes/macrophages to form giant multinucleated cells. *J Exp Me*d. 1988;167:598-611.
[9] Black MM, Epstein WL. Formation of multinucleate giant cells in organized epitheloid cell granulomas. *Am J Pathol*. 1974;74:263–74.
[10] Karimi S, Shamaei M, Pourabdollah M, Sadr M, Karbasi M, Kiani A, et al. Histopathological findings in immunohistological staining of the granulomatous tissue reaction associated with tuberculosis. *Tuberc Res Treat*. 2014;2014:858396. doi: 10.1155/2014/858396.
[11] Gadde PS, Moscovic EA. Asteroid bodies: products of unusual microtubule dynamics in monocyte-derived giant cells. An immunohistochemical study. *Histol Histopathol*. 1994;9:633-42.
[12] Winkelmann RK, Dahl PR, Charles Perniciaro C. Asteroid bodies and other cytoplasmic inclusions in necrobiotic xanthogranuloma with paraproteinaemia. *J Am Acad Dermatol.* 1998;38:967-70.
[13] Gazzoni AF, Severo CB, Salles EF, Severo LC. Histopathology, serology and cultures in the diagnosis of cryptococcosis. *Rev Inst Med Trop Sao Paulo*. 2009;51:255–59.
[14] Baker RD, Haugen RK. Tissue changes and tissue diagnosis in cryptococcosis: a study of twenty-six cases. *Am J Clin Pathol*. 1955;25:14–24.
[15] Sabatine MS, Oelberg DA, Mark EJ, Kanarek D. Pulmonary cholesterol crystal embolization. *Chest*. 1997;112:1687–92.
[16] Horacek J, Horava V. Contribution to differential diagnostics of granulomatous lesions in lung tissue. *Biomed Pap Med Fac Univ Palacky Olomouc Czech Repub*. 2002;146:55-58.
[17] El-Zammar OA, Katzenstein AL. Pathological diagnosis of granulomatous lung disease: a review. *Histopathology*. 2007;50:289-310.
[18] Flórez-Moreno GA, Henao-Ruiz M, Santa-Sáenz DM, Castañeda-Peláez DA, Tobón-Arroyave SI. Cytomorphometric and immunohistochemical comparison between central and peripheral giant cell lesions of the jaws. *Oral Surg Oral Med Oral Pathol Oral Radiol Endod*. 2008;105:625-32.
[19] Anderson S, Shires VL, Wilson A, Mountford AP. Formation of multinucleated giant cells in the mouse lung is promoted in the absence of interleukin -12. *Am J Respir Cell Mol Biol*. 1999;20:371-78.

PARTICULARS OF CONTRIBUTORS:
1. Assistant Professor, Department of Pathology, PES Institute of Medical sciences and Research, Kuppam, Andhra Pradesh, India.
2. Professor, Department of Pathology, Bangalore Medical College and Research Institute, Bangalore, Karnataka, India.
3. Professor, Department of Pathology, Bangalore Medical College and Research Institute, Bangalore, Karnataka, India.
4. Professor, Department of Pathology, Bangalore Medical College and Research Institute, Bangalore, Karnataka, India.

NAME, ADDRESS, E-MAIL ID OF THE CORRESPONDING AUTHOR:
Dr. B.N Kumarguru,
Sri'nivasa, No: 204, 9th Cross, BEML Layout, Basaveshwaranagara, Bangalore- 560079, Karnataka, India.
E-mail: kumarguru1978@yahoo.com

FINANCIAL OR OTHER COMPETING INTERESTS: None.

Date of Submission: **May 28, 2015**
Date of Peer Review: **Jul 29, 2015**
Date of Acceptance: **Sep 03, 2015**
Date of Publishing: **Nov 01, 2015**